3 Radio Observatory and DSN Instrumentation Fundamentals
3.1 Antennas, Antenna Arrays and VLBI

We now want to look at antennas and antenna arrays from a more fundamental point of view. An antenna is a device that effects the transition of an EM wave from one in free space to a guided one in a conductor like a wave guide or a horn. This is called a receiving antenna. It can also effect the transition from a guided EM wave to a free-space wave, In this case it is called a transmitting antenna. The response of an antenna as a function of direction is the antenna beam pattern. The pattern may be expressed in terms of the field intensity (field pattern) or in terms of the pointing vector or radiation intensity (power pattern). The function, $P_n(\theta, \phi)$, that we have used so far is the normalized power pattern. We now want to see how the power pattern is related to the antenna and its electrical potential or aperture distribution.

We distinguish between:

1) near-field pattern --- dependent on angle and distance
2) far-field pattern -- dependent on angle only

In the latter case, the curvature of the wavefront is much less than λ across the geometric dimension of the antenna aperture.

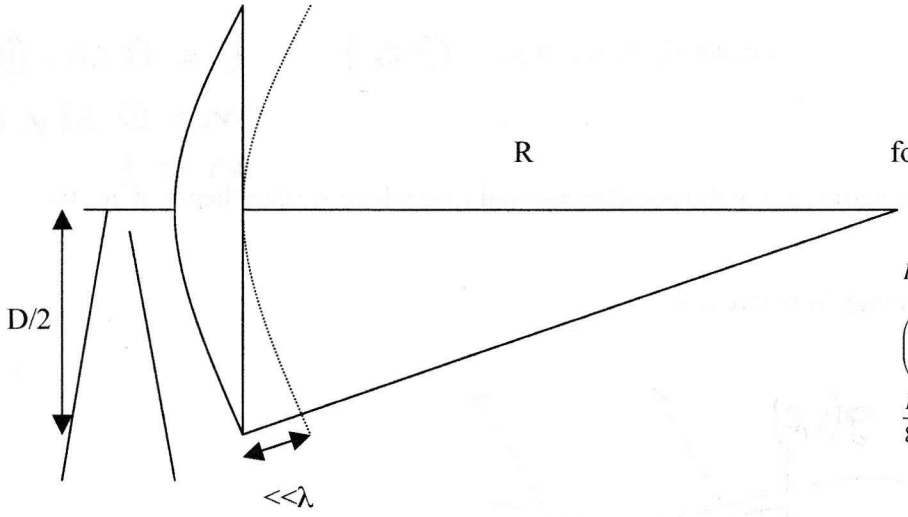

Now let us consider a flat rectangular surface as an antenna which has a particular aperture distribution, g(x,y) and dimensions L_x, L_y.

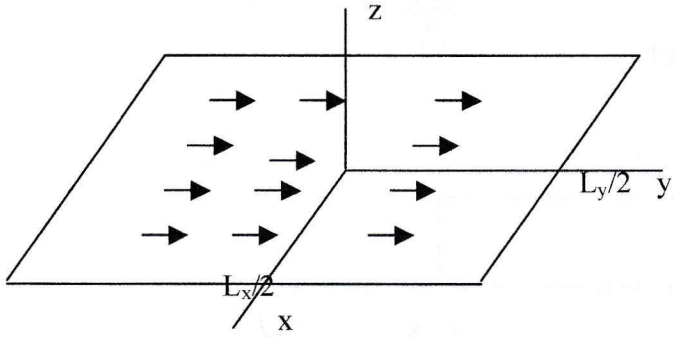

The aperture distribution can be uniform if the surface is illuminated uniformly. It can also have a non-uniform distribution, for instance where the borders are less illuminated.

Now we want to see how the field pattern is related to the aperture and the aperture distribution.

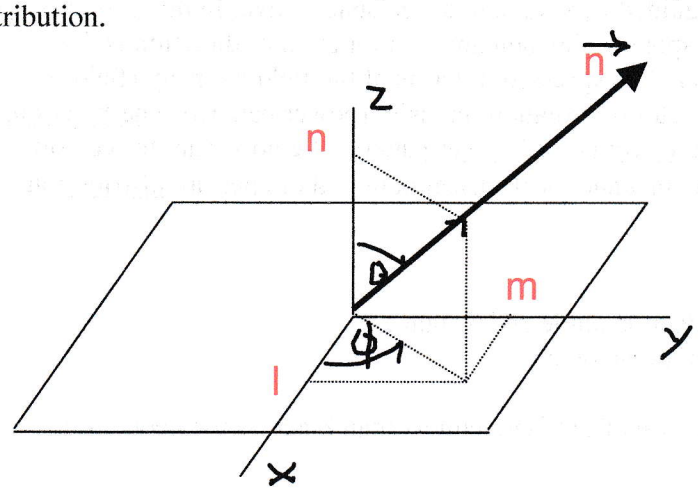

The unit vector of $\vec{n}$ has the components (l, m, n).

$l = \sin\theta \cos\phi$
$m = \sin\theta \sin\phi$
$n = \cos\theta$

if n almost along z, then: $\theta \ll 1$

$l = \theta \cos\phi$
$m = \theta \sin\phi$
$n = 1$

We can illustrate this scenario also in the one-dimensional case where we can then plot g(x,0) more clearly.

A cross-section along x may look like this:

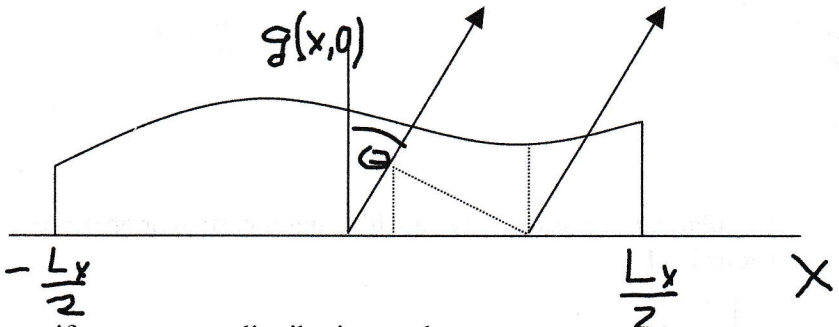

For a uniform aperture distribution we have:

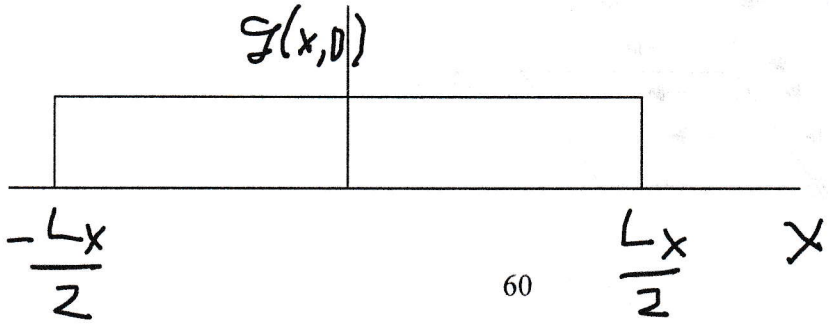

All we want is the far-field pattern in the direction $\bar{n}$. **It can be shown that the far-field pattern, f(l,m), is the FT of the aperture distribution.**

$f(l,m) \Leftrightarrow g(x_\lambda, y_\lambda)$

$$f(l,m) = \iint_{aperture} g(x_\lambda, y_\lambda) e^{-i2\pi(lx_\lambda + my_\lambda)} dx_\lambda dy_\lambda$$

Again, l, m are directional components. The coordinates x_λ, y_λ are called the spatial frequency components, the FT pairs of l, m. They are simply the spatial components, x and y but measured in units of the wavelength λ.

$$x_\lambda = \frac{x}{\lambda}$$

$$y_\lambda = \frac{y}{\lambda}$$

e.g. $x = 100\ m$, $\lambda = 10\ cm$, $x_\lambda = 1000$

For $g(x_\lambda, y_\lambda) = 1$ (uniform aperture distribution we get for a rectangular aperture with length L_x and width L_y:

$g(x_\lambda, y_\lambda) = 1$

$$f(l,m) = \iint_{aperture} 1 e^{i2\pi(lx_\lambda + my_\lambda)} dx_\lambda dy_\lambda$$

$$= \frac{1}{i2\pi l} \frac{1}{i2\pi m} \left[e^{i2\pi l x_\lambda} \Big|_{-\frac{1}{2}\frac{L_x}{\lambda}}^{\frac{1}{2}\frac{L_x}{\lambda}} \right] \left[e^{i2\pi l y_\lambda} \Big|_{-\frac{1}{2}\frac{L_y}{\lambda}}^{\frac{1}{2}\frac{L_y}{\lambda}} \right]$$

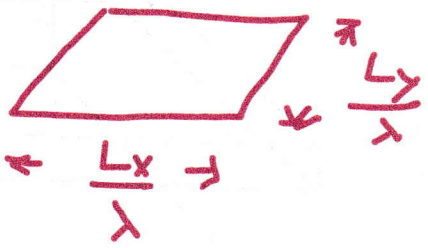

and with

$$\sin x = \frac{1}{2i}\left[e^{ix} - e^{-ix}\right]$$

$$\sin \pi l \frac{L_x}{\lambda} = \frac{1}{2i}\left[e^{i\pi l \frac{L_x}{\lambda}} - e^{-i\pi l \frac{L_x}{\lambda}} \right]$$

$$\frac{1}{i2\pi m}\left[e^{i\pi m \frac{L_y}{\lambda}} - e^{-i\pi m \frac{L_y}{\lambda}} \right]$$

we get

$$f(l,m) = \frac{2}{2\pi l} \frac{2}{2\pi m} \sin \pi l \frac{L_x}{\lambda} \sin \pi m \frac{L_y}{\lambda}$$

$$= \frac{L_x}{\lambda} \frac{L_y}{\lambda} \operatorname{sinc}(l \frac{L_x}{\lambda}) \operatorname{sinc}(m \frac{L_y}{\lambda})$$

The zero-crossings occur where $l\frac{L_x}{\lambda}, m\frac{L_y}{\lambda} = \pm 1, \pm 2. \pm 3....$

$L_\lambda = \frac{L_x}{\lambda}$

$g(x_\lambda) = \Pi\left(\frac{x_\lambda}{L_x/\lambda}\right) = \Pi\left(\frac{x_\lambda}{L_\lambda}\right)$ $\quad f(l) = L_\lambda \, \mathrm{sinc}(lL_\lambda)$

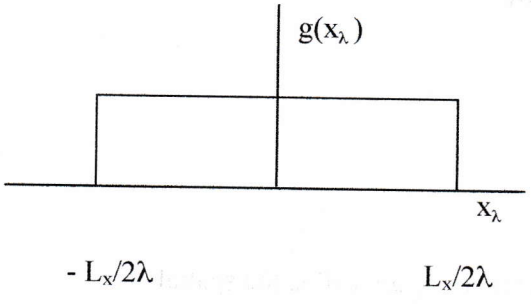

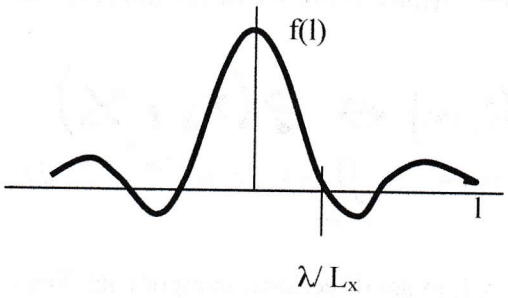

remember:

$\Pi\left(\frac{t}{\tau}\right) \leftrightarrow \tau \, \mathrm{sinc}\left(\frac{\omega\tau}{2\pi}\right)$

For the 2-dim case:

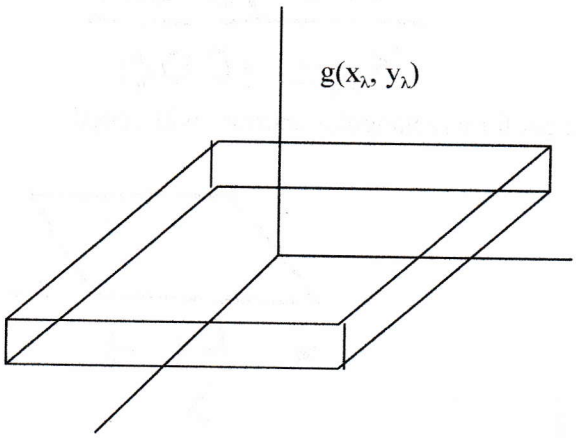

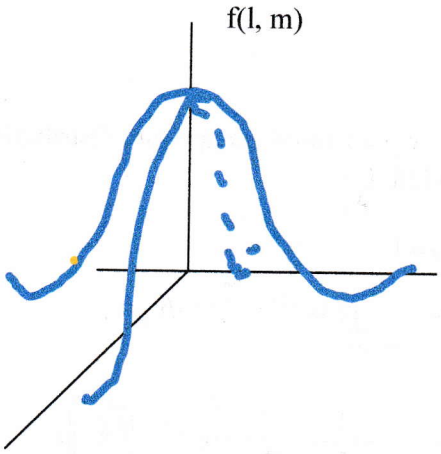

The field pattern f(l, m) determines the angular dependence of the E and H fields. **The beam pattern is simply the normalized power pattern.**

The normalized power pattern, $P_n(\vec{n})$ is given by

$$P_n(\vec{n}) = \frac{|f(\vec{n})|^2}{|f_{\max}|^2}$$

$$P_n(l,m) = \mathrm{sinc}^2(l\frac{L_x}{\lambda})\mathrm{sinc}^2(m\frac{L_y}{\lambda})$$

Remember that l, m are functions of θ, ϕ.

Examples of rectangular apertures:

Array of dipoles

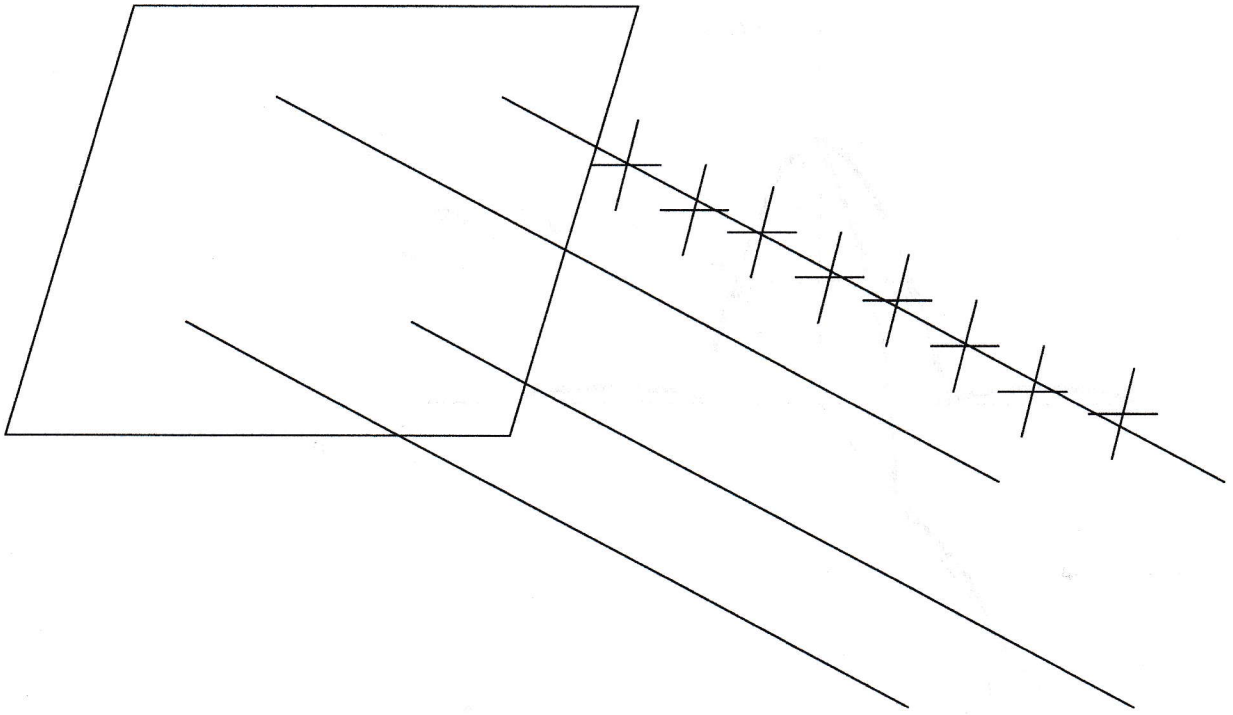

Horn antenna

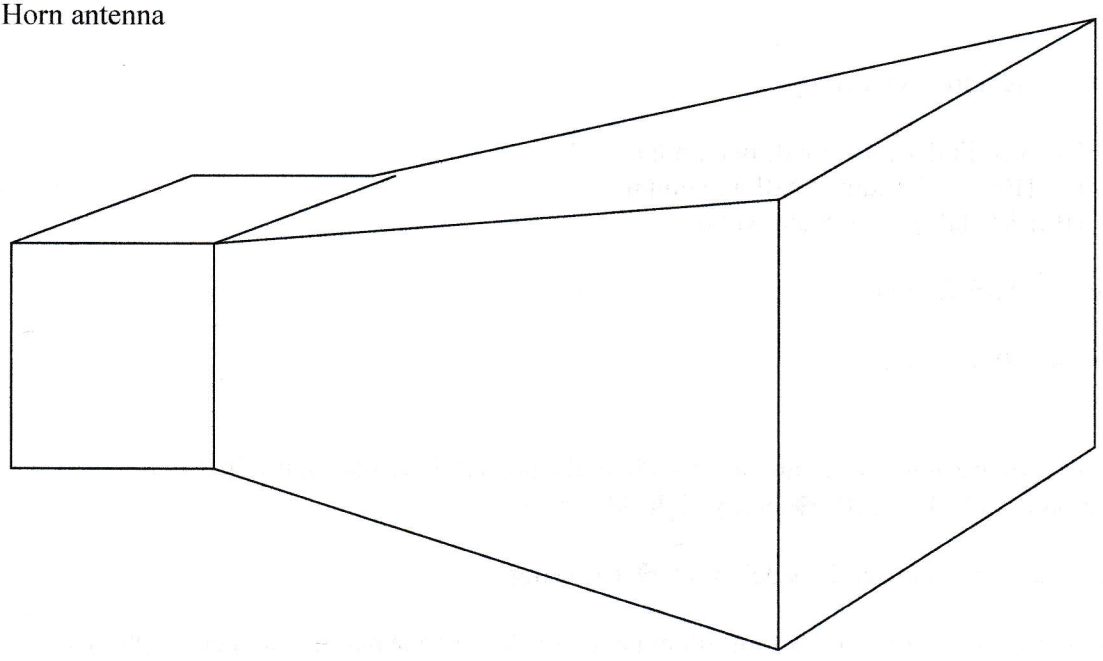

If we plot the beam pattern, $P_n(l,m)$, in two dimensions, it looks like this:

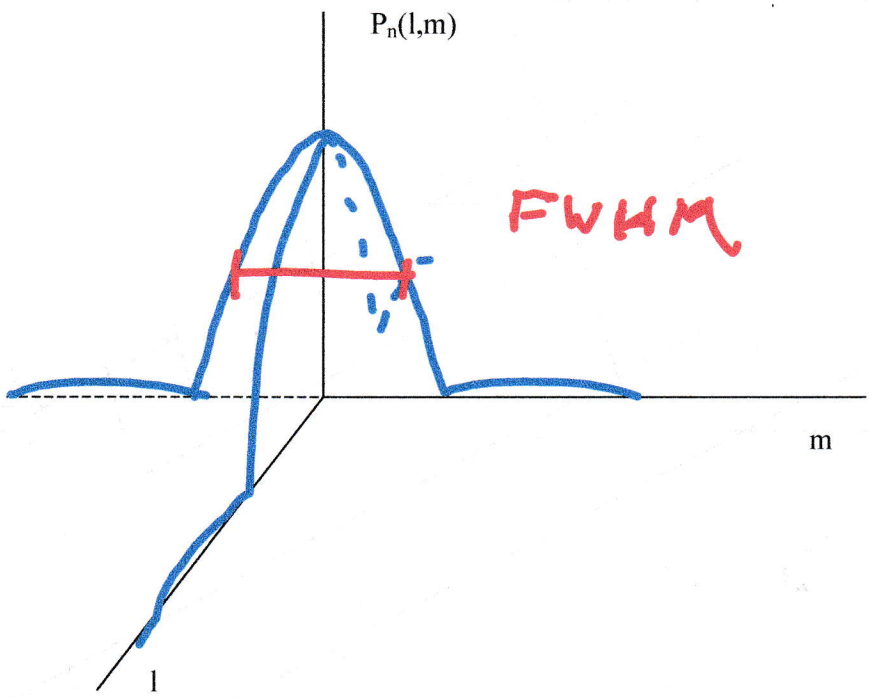

Here are some important acronyms:

FWHM: Full-width at half maximum
HWHM: Half-width at half maximum
HPBW: Half power beam width

$FWHM_x \sim 0.88\ \lambda/L_x$ rad

$FWHM_y \sim 0.88\ \lambda/L_y$ rad

First sidelobes are at $\pm 1.4\lambda/L_x$ and have 4.7% of the power along boresight. That is an attenuation of only 13.3 dB! ➔ pretty high sidelobes!

What can be done to lower the sidelobes? ➔**Tapering**

Tapering is a way to use non-uniform illumination of the antenna aperture and de-emphasize illumination of the borders of the aperture.

Tapering:

We can modify the aperture distribution and see how the power pattern (beam pattern) changes. From an engineering point of view, modifying the aperture distribution is accomplished by modifying the illumination of the aperture of the antenna through the feed in the focal area. This is called **"tapering"** if the illumination is lower at the boarders of the antenna aperture. We will now use a particular modification of the uniform aperture distribution to illustrate tapering and its effect on the filed pattern and beam pattern. We will use the knowledge we gained so far in mathematically deriving the field patterns for particularly tapered aperture distributions. For simplicity, we will just look at the 1-dim case.

Example: Triangularly shaped $g(x_\lambda)$
For simplicity, we want to indicate only the shape of the functions and ignore constants like L_x/λ and 2π. On the left side we plot the aperture distribution, $g(x_\lambda)$ and on the right side we plot the filed pattern, f(l).

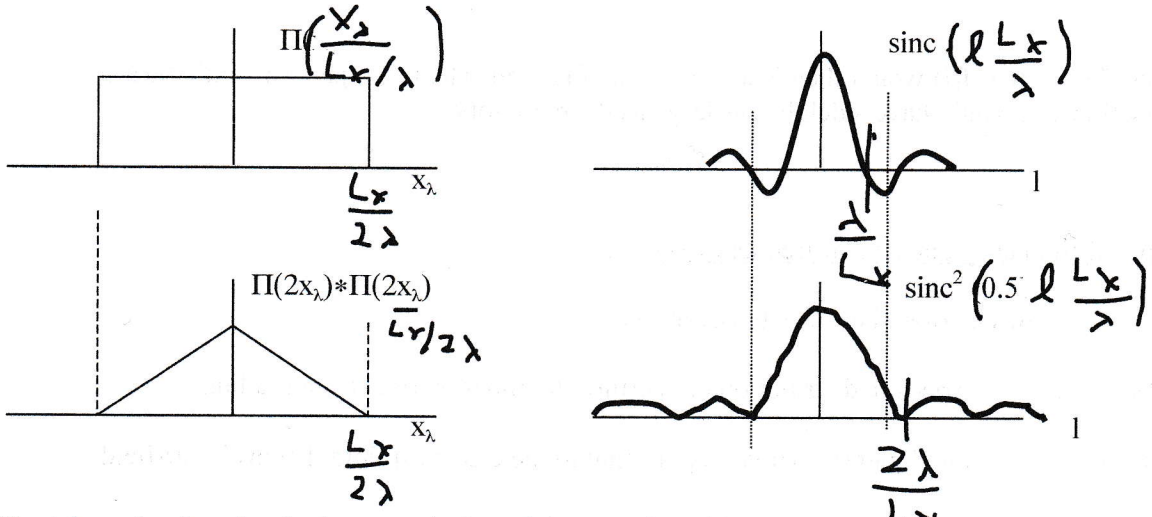

The triangular function is the convolution of the gate function. But it is twice as broad as the gate function. If we narrow the width of the triangular function by a factor 2, then the $sinc^2$-function broadens by a factor 2. But the sidelobes are also much lower. When we then calculate the beam pattern P_n (l), we see that tapering had the effect of lowering the sidelobes and broadening the beam.

What happens if we inverse the taper?

Example; $g(x_\lambda)$ with $g(x_\lambda) * g(x_\lambda) = \Pi(x_\lambda)$

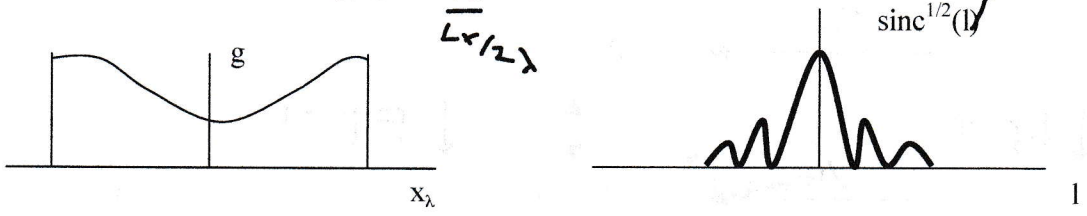

In this case, FT{g} is the square root of the sinc-function. The main lobes would get narrower and the sidelobes higher.

In the extreme case, $g(x_\lambda)$ could develop into δ-functions.

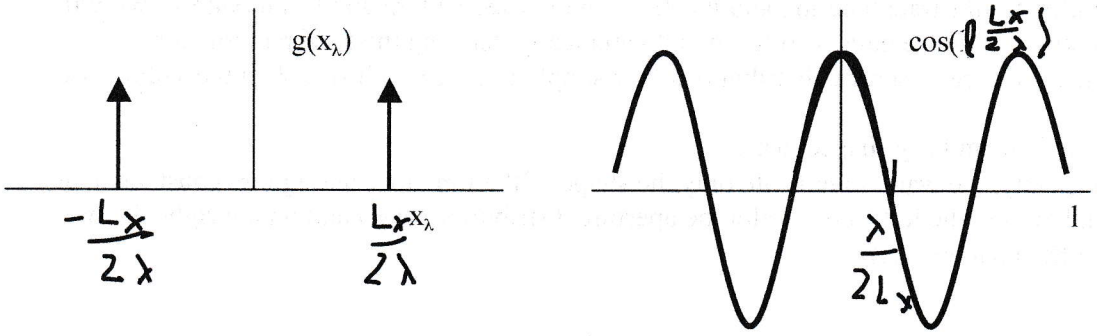

The field patter, f(l) would then just be a cosine function. The beam pattern would be a $\cos^2$ – function and would have sidelobes as large as the main lobe.

Spatial frequency and spatial frequency spectrum

We have now elaborated quite extensively on:

$g(x_\lambda, y_\lambda)$: Aperture distribution or aperture illumination or current grading

f(l,m) : Field pattern (it is proportional to the electrical field, E(l,m) in far-field

$P_n(l,m)$: Antenna power pattern or beam pattern or angular power spectrum

We now introduce a new function:

$\overline{P}_n(x_\lambda, y_\lambda)$: FT{$P_n(l, m)$}: Spatial frequency spectrum or spatial frequency response

In symbolic representation we have now:

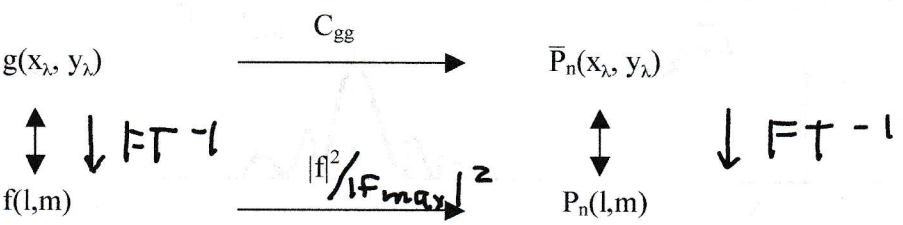

x_λ : spatial frequencies

To visualize these functions, we plot them for a specific 1-dim case:

aperture distribution

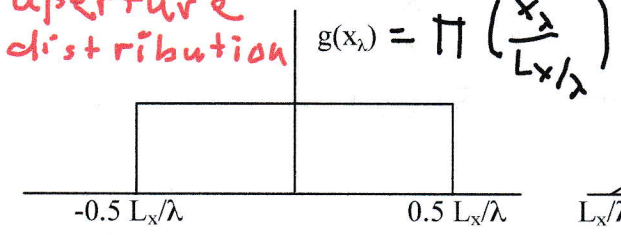

Spatial frequency response

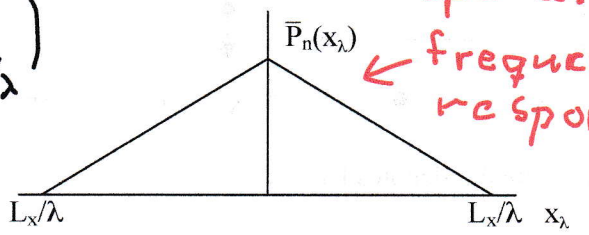

field pattern

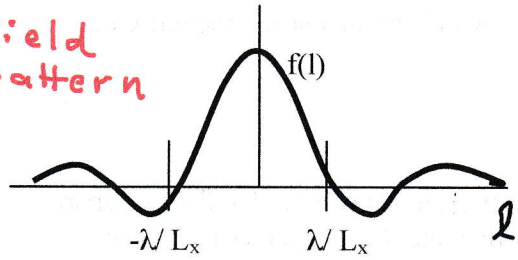

antenna beam pattern

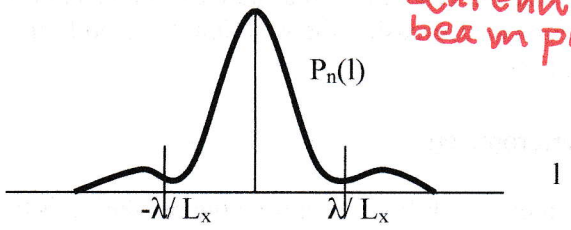

The analogy to signals as a function of time is apparent. However, there is a slight break with the analogy. $|F(\omega)|^2$ is called energy density spectrum, but $P_n(l)$ is called antenna power pattern or antenna beam pattern.

The analogy goes further. For a uniform aperture distribution, we get a triangularly-shaped spatial frequency spectrum or spatial frequency response from $x_\lambda=0$ to L_x/λ . We say that the antenna has low-pass spatial frequency filter characteristics. Its sensitivity is maximum for spatial frequencies = 0 and decreases linearly with increasing spatial frequency up to a maximum spatial frequency of L_x/λ . Larger spatial frequencies are not passed through the antenna. In fact, the antenna is a linear spatial filter. We can sketch the analogy in the following way;

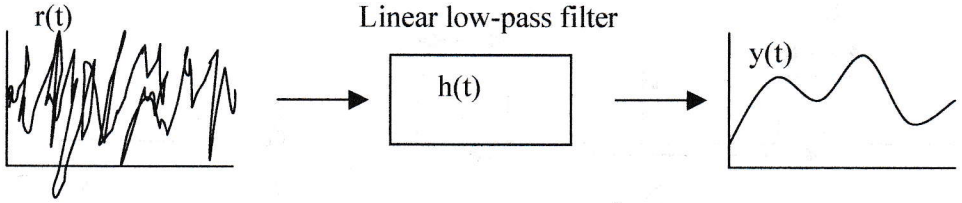

symmetric

$P_n(\theta) = \bar{P}_n(\theta)$

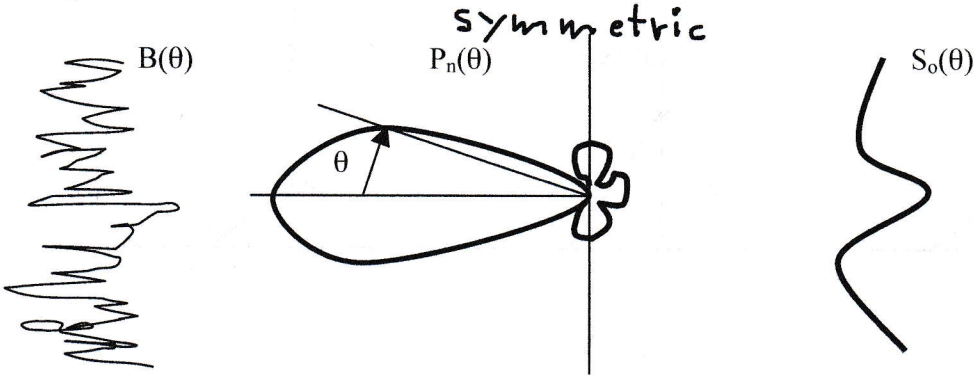

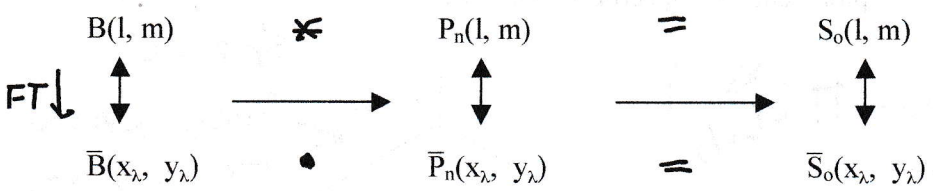

where the bar denotes FT.

Tha angular resolution of a radio antenna can be increased by increasing the size of the antenna or decreasing the wavelength or both; in other words, by increasing the ratio, L_x/λ and L_y/λ.

Interferometers

Another possibility to improve the resolution is to use two antennas spaced a distance apart. Below we have sketched a pair of antennas, each of diameter L and spaced a distance, s, apart.

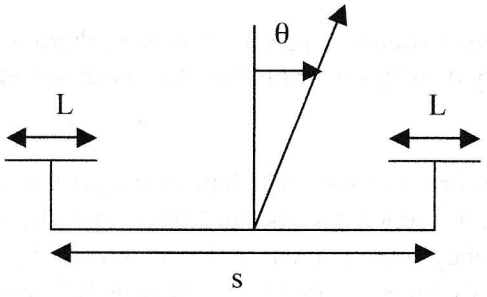

$l = \sin\theta\cos\phi$
for $\theta \ll 1$, $\phi = 0$
$l = \theta$

If the antennas have uniform aperture distributions, the spatial frequency response, $\bar{P}_n(x_\lambda)$, can be readily computed. We just want to look at the 1-dim case along the x-axis.

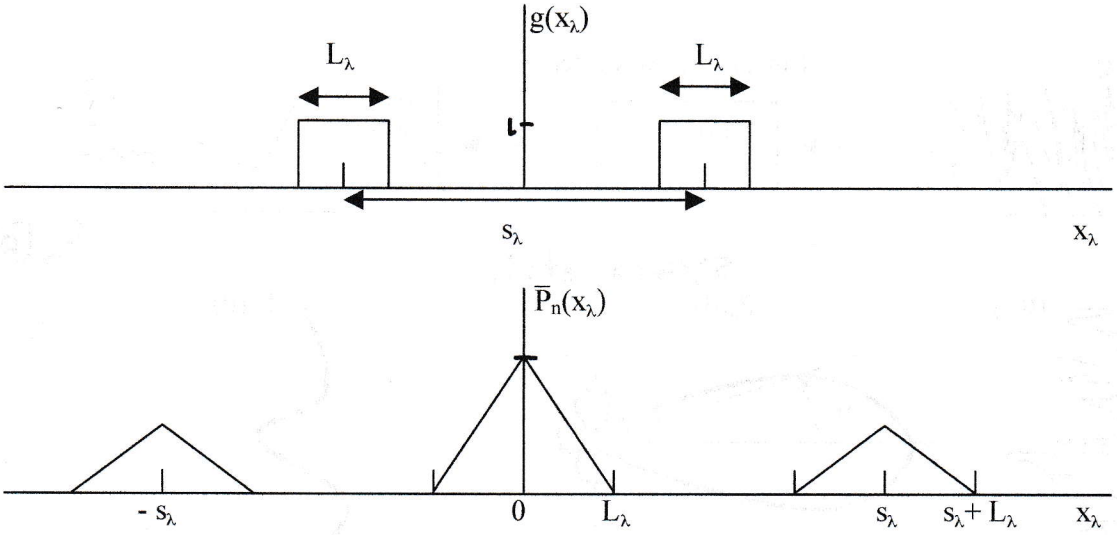

Here,
$L_\lambda = L/\lambda$
$s_\lambda = s/\lambda$

Now we want to compute the field pattern f(l) and the beam pattern or angular power pattern, $P_n(l)$. Rather than computing the FT directly with a lot of sweat, we represent $g(x_\lambda)$ as the convolution of the gate function, $\Pi(x_\lambda / L_\lambda)$, and a pair of spaced delta functions, $\delta(x_\lambda + s_\lambda/2) + \delta(x_\lambda - s_\lambda/2)$. The field pattern is then the product of the FT of the individual functions.

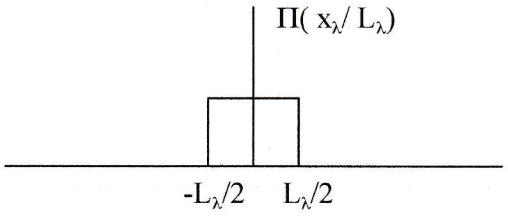

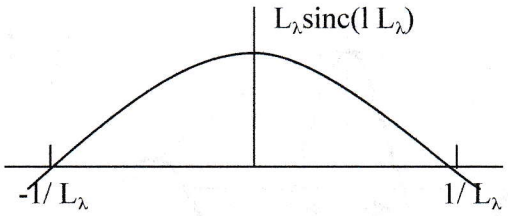

*

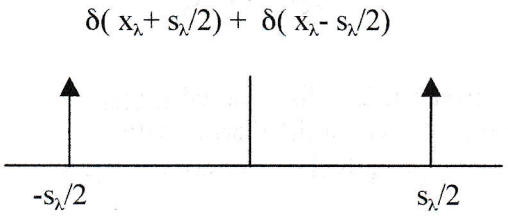

●

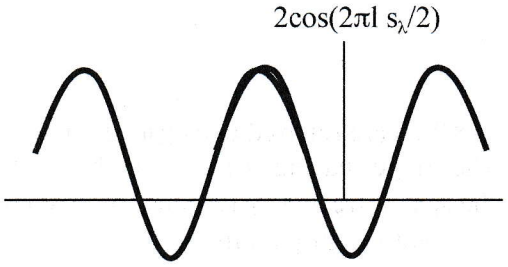

=

=

$\Pi[\frac{x_\lambda}{L_\lambda} + \frac{s_\lambda}{2}] + \Pi[\frac{x_\lambda}{L_\lambda} - \frac{s_\lambda}{2}]$

$2L_\lambda \text{sinc}(l L_\lambda)\cos(2\pi l s_\lambda/2)$

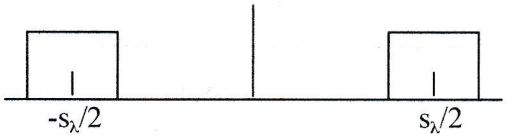

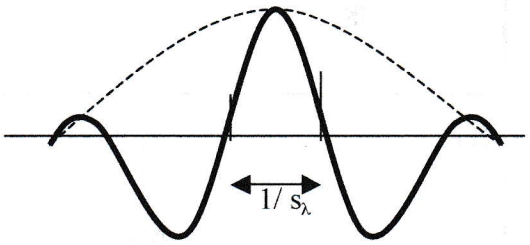

All four functions can be sketched as follows:

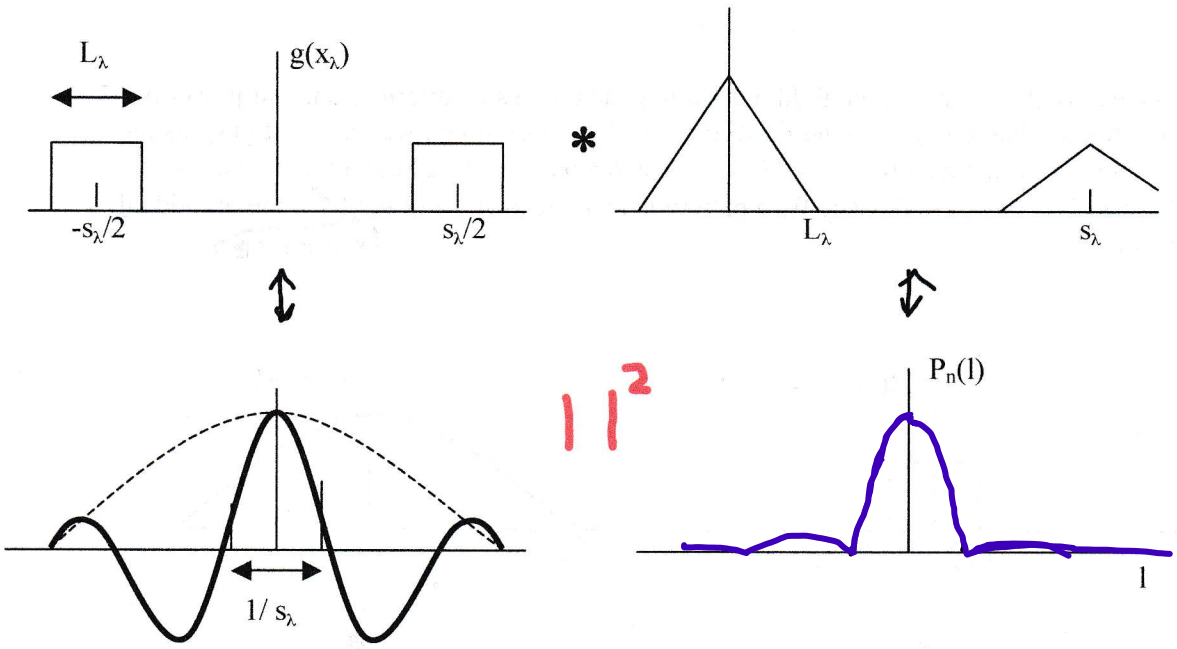

The lobes in $P_n(l)$ are referred to as <u>fringes.</u> The width between first nulls is called <u>fringe spacing</u>. The fringe spacing is $1/s_\lambda$, which is ½ $1/L_\lambda$ compared with a filled array with $s_\lambda = L_\lambda$. The spatial frequency response of this interferometer is equivalent to a combination of a low-pass and a high-pass filter.

What is the output of such interferometer when sources of different brightness distributions are observed?

For a point source we get:

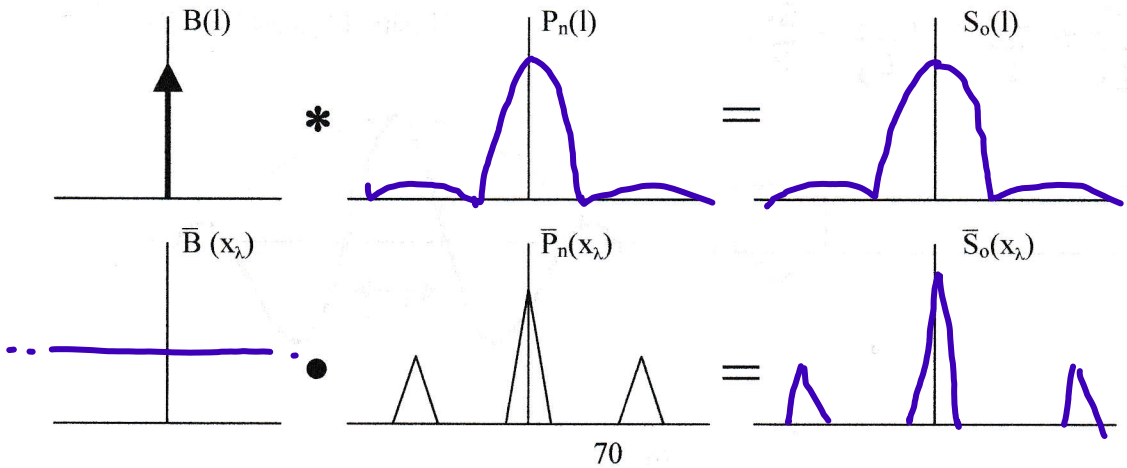

For a source that is a bit more extended but with a diameter, α, still smaller than, or equal to, the lobe spacing, $1/s_\lambda$, with $\alpha \leq 1/s_\lambda$, we get;

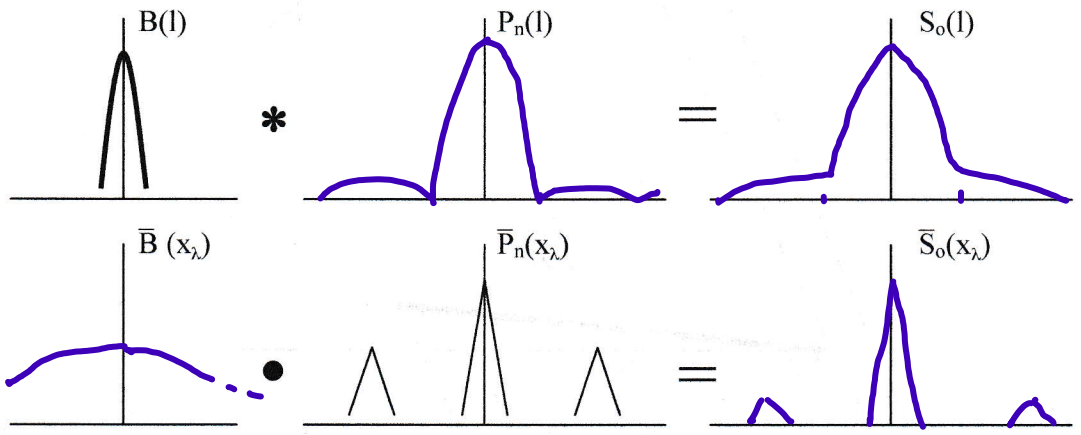

Clearly, the high frequency component of $\bar{S}_o(x_\lambda)$ is distorted and smaller. This is equivalent to a smoothing of $\bar{S}_o(x_\lambda)$. The degree of smoothing of the fringes depends on the extent of the source. If we increase the source size to $\alpha \geq 1/s_\lambda$, then fringes get smaller and if the source is really large, then fringes can hardly be seen anymore till they completely vanish with further increasing source size.

The geometry of an elementary interferometer can be sketched as follows.

Here, D, is the baseline, $D\sin\theta = c\tau_g$, where c is the speed of light and τ_g is the geometric delay. The outputs of the two antennas are amplified, multiplied, and integrated over time, in principle. This is done mainly in the correlator. But we will get to it later.

The coordinate system for the baseline vector is chosen such that D is expressed in units of λ, $\vec{D}_\lambda = \frac{\vec{D}}{\lambda}$ (in our previous 1-dim case, this corresponds to s_λ) and $D_\lambda = (u, v, w)$.

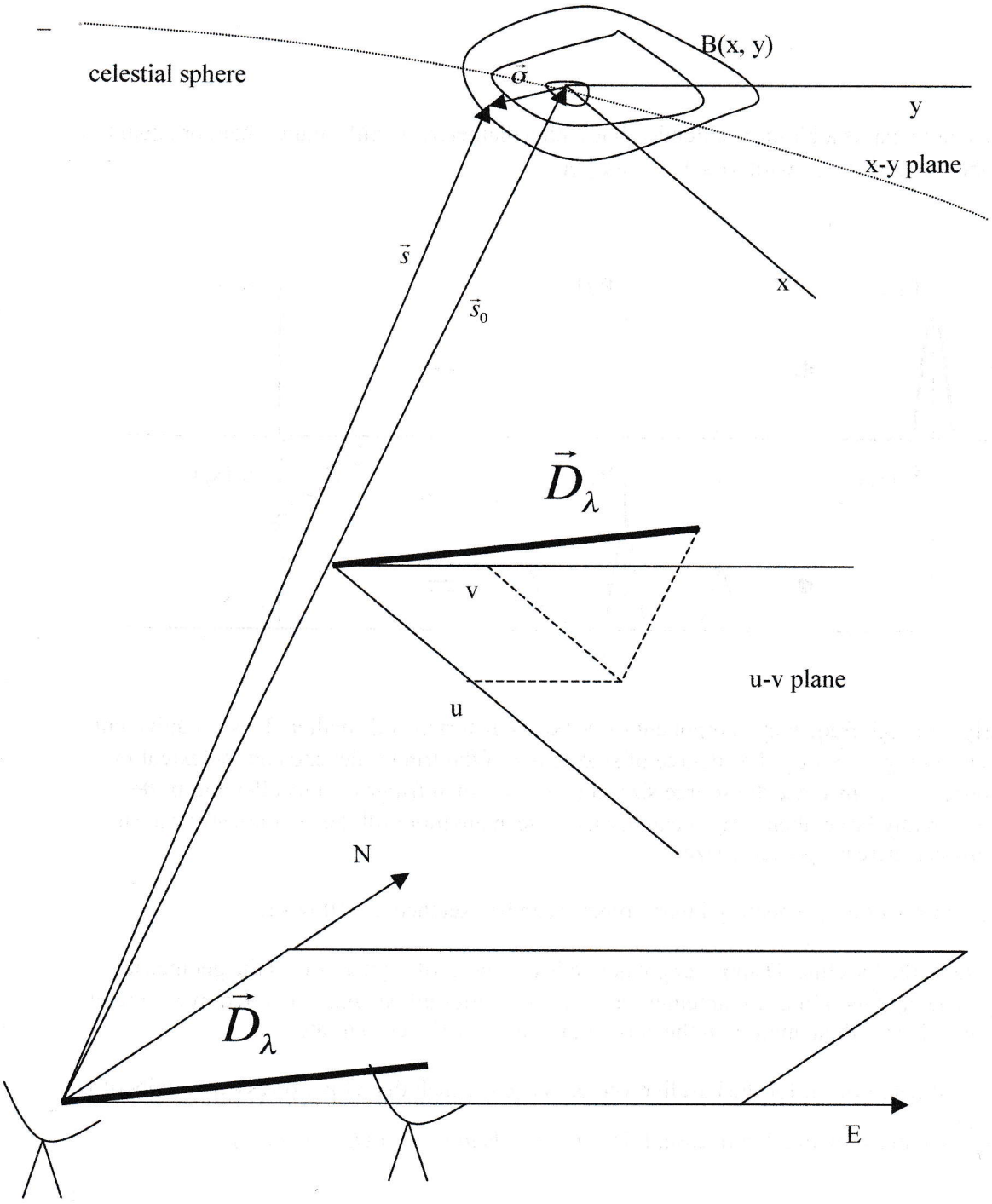

$\vec{s}_0$: Vector of source center (phase center which structure phase is referred to)

$\vec{s}$: Vector to slightly different direction in brightness distribution of source.

$\vec{\sigma}$: Difference vector, $\vec{s} - \vec{s}_0$

u : Component of $\vec{D}_\lambda$ in plane perpendicular to $\vec{s}_0$. It points to local east.

v : Component of $\vec{D}_\lambda$ in plane perpendicular to $\vec{s}_0$. It points to local north.

x-y plane: Tangent plane on the celestial sphere with the tangent point being the origin at $\vec{s}_0$, the phase center

The angular distance from any point in the map from the origin of the coordinate system is proportional to the sine of the corresponding angle on the sky. If the angle is small, as it is usually in interferometry, then the sine of the angle is equal to the angle (in rad). Assuming a small extension of the brightness distribution, one can show that:

$$\vec{D}_\lambda \bullet \vec{s}_0 = ux + vy$$
$$d\vec{\sigma} = dxdy$$

The projection of the baseline vector on the u-v plane changes as the earth rotates. As a result, the projection of $\vec{D}_\lambda$ traces ellipses on the u-v plane.

For an array of antennas, say N antennas, we get N(N-1) independent ellipses. A uniform distribution of ellipse would be ideal and would be equivalent to a uniform aperture distribution over a very large area. In reality, the aperture distribution is far from uniform and results in complicated sidelobes of the interferometer array's power pattern or beam pattern. Tapering could diminish the sidelobes to some degree, but the FWHM of the beam pattern would broaden at the expense of resolution power. The challenge in the analysis of data from arrays is to cope with the complicated aperture distribution.

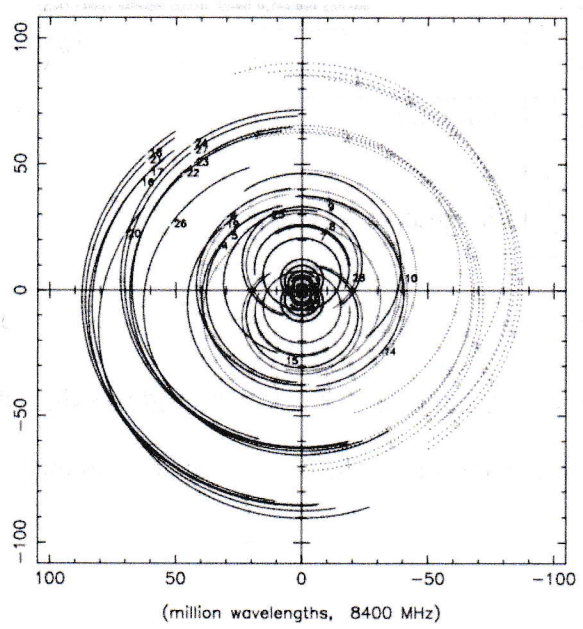

Now we want to go a step further and see how the signal is received by an interferometer of two antennas and then correlated.

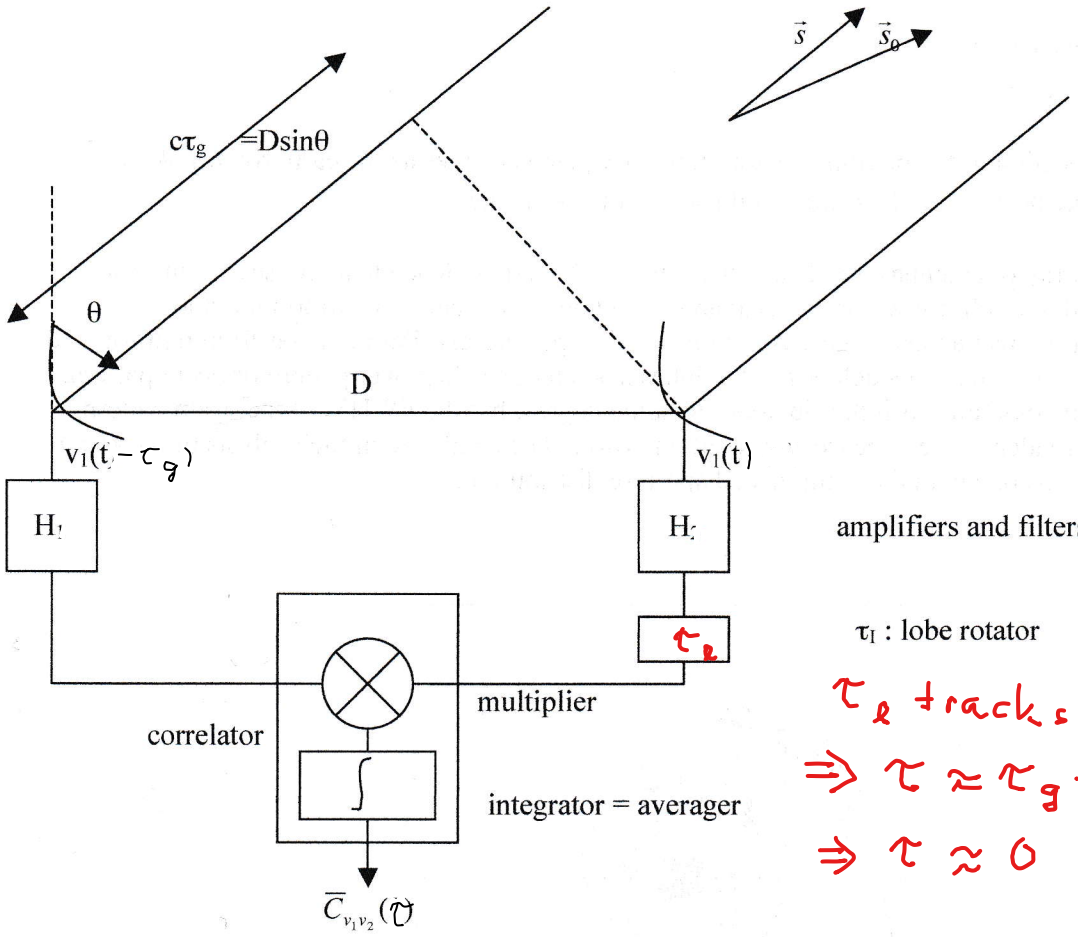

τ_I tracks τ_g

$\Rightarrow \tau \approx \tau_g - \tau_I \ll \tau_g$

$\Rightarrow \tau \approx 0$

The correlator output for a point source as a function of the filter bandpass characteristics

Let us assume that we are observing a point source and that the signal from that source is a plane wave with:

$V_1(t) = Ee^{i\omega t}$

$V_2(t) = Ee^{i\omega(t-\tau_g)} = v_1(t-\tau_g)$

The two amplifier-filter combinations, H_1 and H_2, are assumed to have identical bandpass characteristics, that is identical transfer functions with $H_1 = H_2 = H$. The integration time is on the order of 1s, which is 10^7 times larger than $1/\Delta\nu$, if the bandwidth of the filters, $\Delta\nu$, is 10 MHz. For all practical purposes that means that the integration goes from – infinity to +infinity.

If we assume that the transfer functions are rectangular in magnitude, that is, the filters have ideal filter characteristics, i.e. a rectangular bandpass, then

$$H(\omega) = \Pi\left(\frac{\omega}{\Delta\omega}\right) * [\delta(\omega+\omega_0) + \delta(\omega-\omega_0)]$$

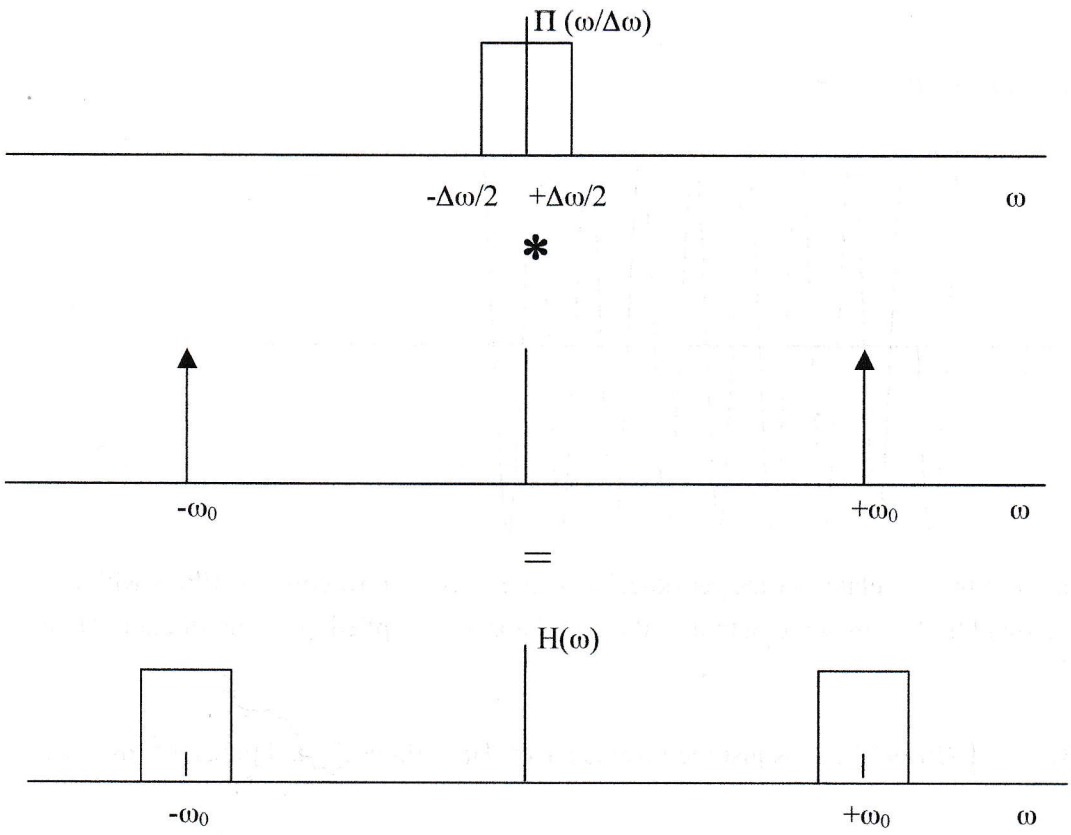

The output of the correlator is:

with $H(\omega) = H^*(\omega)$ and $H^2(\omega) = H(\omega)$

$$\overline{C}_{V_1V_2}(\tau) = \lim_{\tau\to\infty}\frac{1}{T}\int_{-T/2}^{+T/2}\int_{-\infty}^{+\infty} E^2 H(\omega)e^{i\omega t}e^{-i\omega(t-\tau_g+\tau)}d\omega dt$$

Let us first do the integration over time:

$$\overline{C}_{V_1V_2}(\tau) = \lim_{\tau\to\infty}\frac{1}{T}\int_{-T/2}^{+T/2}\int_{-\infty}^{+\infty} E^2 H(\omega)e^{i\omega(\tau_g-\tau)}d\omega dt$$

$$= E^2\int_{-\infty}^{+\infty} H(\omega)e^{i\omega(\tau_g-\tau)}d\omega$$

And for $\tau = 0$:

$$\overline{C}_{V_1V_2}(0) = E^2\int_{-\infty}^{+\infty} H(\omega)e^{i\omega\tau_g}d\omega$$

For the case with infinitely narrow bandpass filters we get

$$\overline{C}_{V_1V_2}(0) = E^2\int_{-\infty}^{+\infty}[\delta(\omega+\omega_0)+\delta(\omega-\omega_0)]e^{i\omega\tau_g}d\omega$$

$$= 2E^2\cos(\omega_0\tau_g)$$

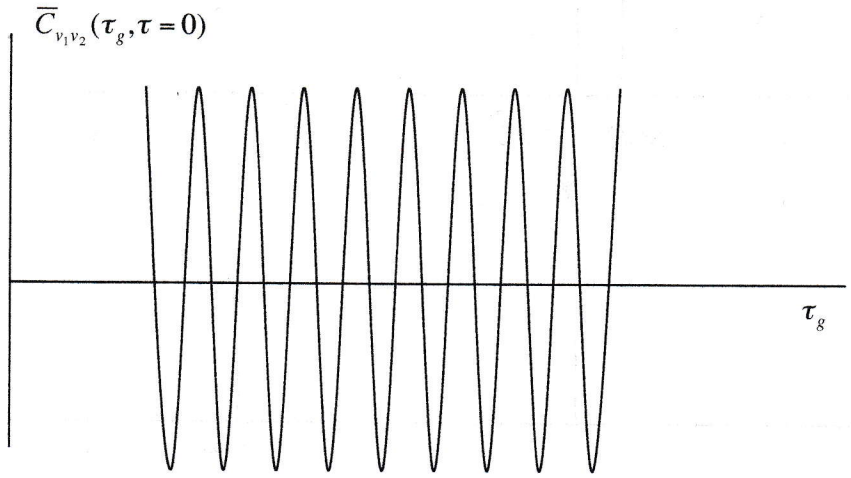

The output of the correlator varies periodically with τ_g. If we now consider filters with a finite bandwidth, $\Delta\omega$, then the output of the correlator is multiplied by a sinc finction. Here is why:

$\overline{C}_{V_1V_2}(0) = E^2\int_{-\infty}^{+\infty} H(\omega)e^{i\omega\tau_g}d\omega$ is just the inverse FT of H(ω) times 2π and times E^2. In other words,

$$\overline{C}_{V_1V_2}(0) = 2\pi E^2\left[FT^{-1}\left\{\Pi\left(\frac{\omega}{\Delta\omega}\right)*\delta(\omega+\omega_0)+\Pi\left(\frac{\omega}{\Delta\omega}\right)*\delta(\omega-\omega_0)\right\}\right]$$

$$= 2\pi 2\pi E^2 FT^{-1}\Pi\left(\frac{\omega}{\Delta\omega}\right)\left[FT^{-1}(\delta(\omega+\omega_0)+\delta(\omega-\omega_0)\right]$$

$$= 2\pi 2\pi E^2\frac{\Delta\omega}{2\pi}\frac{\sin\frac{\Delta\omega}{2}\tau_g}{\frac{\Delta\omega}{2}\tau_g}\frac{2}{2\pi}\cos\omega_0\tau_g$$

$$= 2E^2\Delta\omega\,\mathrm{sinc}\left(\frac{\Delta\omega}{2\pi}\tau_g\right)\cos\omega_0\tau_g$$

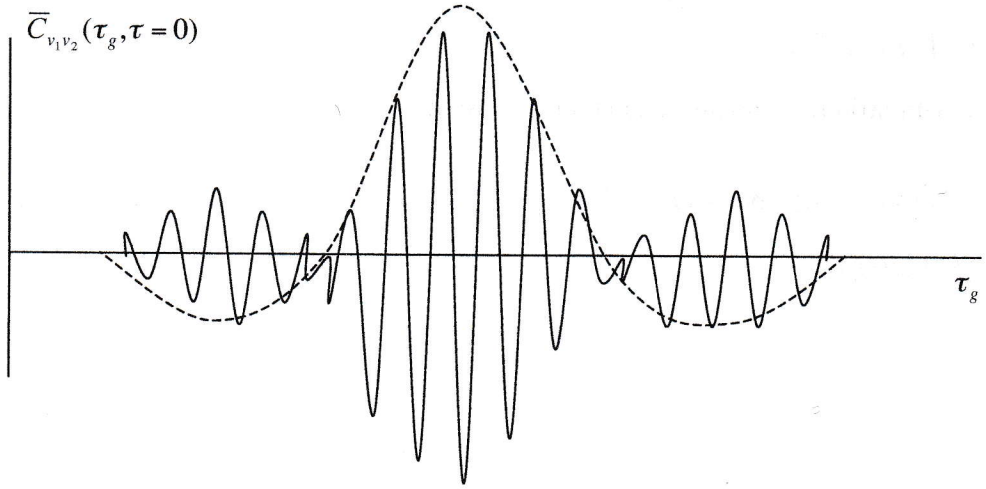

Envelope zero crossings at

$$\frac{\Delta\omega}{2\pi}\tau_g = \pm 1, \pm 2 \ldots$$

$$\tau_g = \pm\frac{2\pi}{\Delta\omega}, \pm\frac{4\pi}{\Delta\omega}$$

If the transfer functions of the filters are not rectangular, then $\overline{C}_{V_1V_2}(0)$ assumes, instead of the sinc-function a different term. For instance, if the transfer function is a Gaussian, then the sinc term is replaced by a Gaussian.

The envelope is often called "delay pattern or bandwidth pattern or fringe washing function.

Usually, the delay is tracked with the lobe rotator so that $\tau = \tau_g - \tau_i$ is very small, that is close to 0. That is why we were interested in $\overline{C}_{V_1V_2}(\tau = 0)$. However, τ_i, has to be computed and applied before correlation. It is computed for a nominal position of the source at the sky that is believed to be the correct position of the source. This position is referred to as $\vec{s}_0$. The lobe rotator continuously applies updated values of τ_i as the Earth rotates and the baseline vector components, u and v, change.

The correlator output for an extended source

We now want to consider the correlator output as a function of the brightness distribution, $B(\vec{s})$, of the source at the sky. In particular, we want to look at the part $R(\vec{D})$ with

$$\overline{C}_{v_1v_2}(0) = \int_{-\infty}^{+\infty} H(\omega)R(\vec{D})d\omega$$

In other words, we want to ignore the integration over the filter bandwidth.

The electrical filed squared, E^2, is proportional to B for a point source. For an extended source we have to "add" all point sources, that means we have to integrate over the extend of the source.

$$R(\vec{D}) = \iint_{source} B(\vec{s})e^{i\omega\tau_g}d\vec{s}$$

Since

$$\tau_g = \frac{1}{c}\vec{D}\bullet\vec{s}$$

and

$$\vec{s} = \vec{s}_0 + \vec{\sigma}$$

we can write

$$R(\vec{D}) = \iint_{source} B(\vec{s}_0 + \vec{\sigma})e^{i\frac{\omega}{c}\vec{D}\bullet(\vec{s}_0+\vec{\sigma})}d(\vec{s}_0 + \vec{\sigma})$$

We now use a particular coordinate system for B that is centered at $\vec{s}_0$. Also, in interferometry, the sources are not much extended around $\vec{s}_0$, so that $\vec{\sigma}$ is always rather small. With now $B = B(\vec{\sigma})$ we get

$$R(\vec{D}) = e^{i\frac{\omega}{c}\vec{D}\bullet\vec{s}_0} \iint_{source} B(\vec{\sigma}) e^{i\frac{\omega}{c}\vec{D}\bullet\vec{\sigma}} d(\vec{\sigma})$$

Here

$e^{i\frac{\omega}{c}\vec{D}\bullet\vec{s}_0}$ is an oscillating function for a nominal direction, $\vec{s}_0$, and

$\iint_{source} B(\vec{\sigma}) e^{i\frac{\omega}{c}\vec{D}\bullet\vec{\sigma}} d(\vec{\sigma})$ is called the visibility function.

$R(\vec{D})$ now consists of an oscillating term for a nominal direction $\vec{s}_0$ which varies with the changing projected baseline as the earth rotates. When we integrate this term over the bandwidth of the filter, we get the oscillating term (sinc times cos) we considered before.

The second term describes the structure or brightness distribution of the source. Again, it is the visibility function with

$$V(\vec{D}_\lambda) = \iint_{source} B(\vec{\sigma}) e^{i2\pi\vec{D}_\lambda\bullet\vec{\sigma}} d(\vec{\sigma})$$

With coordinates, x and y, for $\vec{\sigma}$ at the sky and

$$\frac{\omega}{c}\vec{D}\bullet\vec{\sigma} = \frac{2\pi}{\lambda}\vec{D}\bullet\vec{\sigma} = 2\pi\vec{D}_\lambda\bullet\vec{\sigma} = 2\pi(ux+vy)$$

$\omega = 2\pi\nu = 2\pi\frac{c}{\lambda}$

Compare with:

$$f(t) = \frac{1}{2\pi}\int_{-\infty}^{+\infty} F(\omega) e^{i\omega t} dt = \int F(\nu) e^{i2\pi\nu t} dt$$

$$F(\omega) = \int f(t) e^{-i\omega t} dt$$

$$F(\nu) = \int f(t) e^{-i2\pi\nu t} dt$$

we can now write

$$V(u,v) = \iint_{source} B(x,y) e^{i2\pi(ux+vy)} dxdy$$

$$B(x,y) = \iint_{source} V(u,v) e^{-i2\pi(ux+vy)} dudv$$

Note: Compare 2πux and 2πvy with 2πνt=ωt, and we can understand why u, v are called spatial frequency components.

Example:

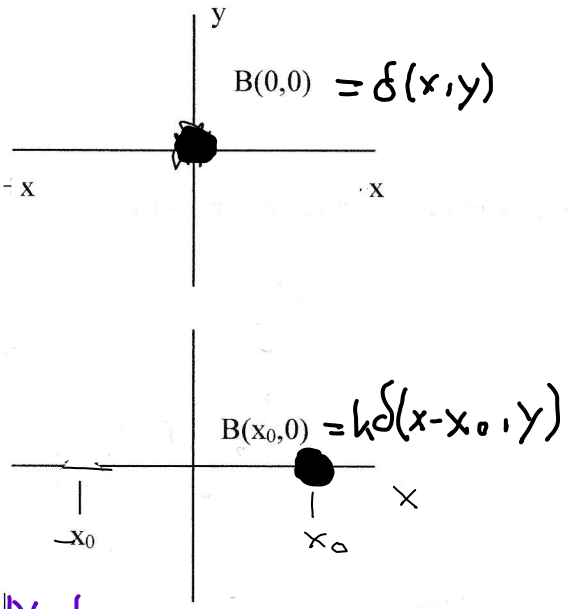

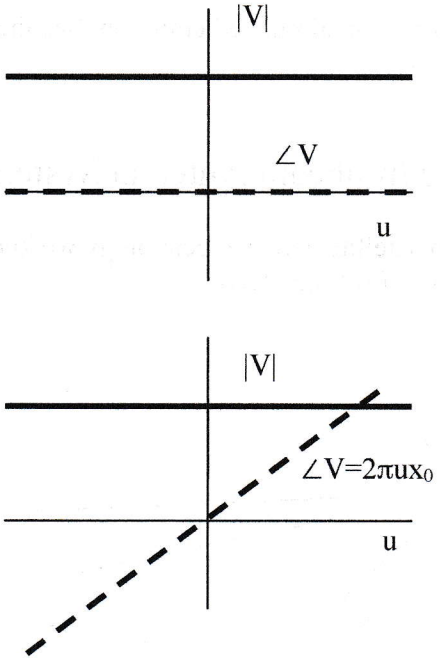

Note: x and u axes are usually reversed

D|=10,000 km
λ = 1 cm
$u_{max} = 10^9\lambda$, assuming that $|D|/\lambda = u_{max}$
x_0 = 10 μas = 4.848 10^{-11} rad
➔
$\angle V = 2\pi u_{max} x_0 = 2\pi\ 4.848\ 10^{-2}\ 360/2\pi$ deg = 17 deg

We can measure such phase in the visibility function and then determine x_0 accurately. How accurately? x_0 = 10 μas corresponds to 36 m at the distance of Jupiter! Hyper accurate spacecraft navigation possible!

However, this measurement of phase at u_{max} = is only reliable if it can be determined unambiguously. With only a 2-element interferometer and only a short measurement for say, 10 min, where the projected baseline does not change very much, the measurement of phase is ambiguous by n2π. In fact the measurement of phase could also be 17 +360 deg or 17 -360 deg. These ambiguities correspond to different fringes of the response of the interferometer. Only the width of the envelope of the oscillating function, the sinc-function, limits the range for the number of ambiguities. That is why we need an array of telescopes that gives us many baselines and many points in the u-v plane. With many points, the phase can be unambiguously determined. And that means that the position offset x_0, can also be unambiguously determined.

3.2 Time and Frequency Standards

A prerequisite of interferometers is that clocks at the antenna sites are extremely well synchronized. For this purpose, hydrogen masers are used. Hydrogen masers are the most stable clocks over short time intervals, namely over a few days or so. A maser is based on the

principle of stimulated emission. See the description on the sheets handed out in class.

3.3 Multibeam Antenna Systems

From satellite antenna technology we know that multi beams can be produced by using a cluster of off-axis feeds.

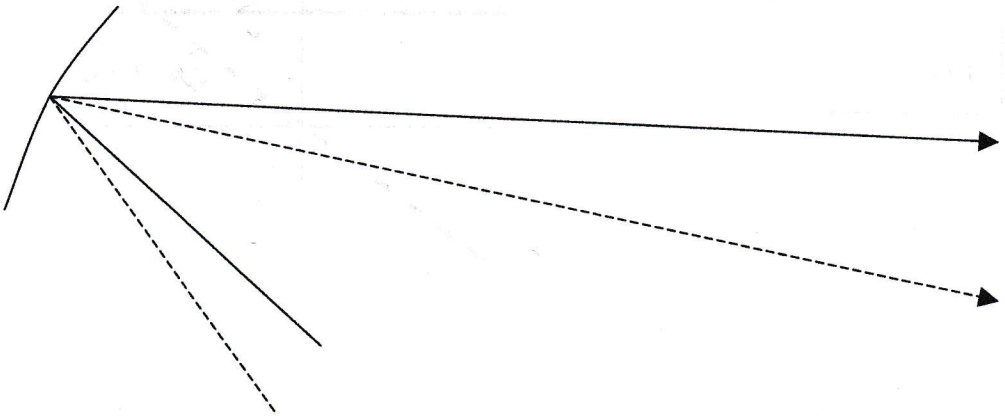

Each feed-reflector combination has its own beam pattern with a main lobe and with side lobes. This technology is used to produce several spot beams covering particular areas on the globe.

Horn clusters are also used in radio astronomy. An example of a horn cluster is given below. Shown are three round horns each producing beams with FWHM, θ. This arrangement produces a wider field of view (FoV) than what is obtained with just one feed. In effect, a cluster of feed horns provides a multi-pixel imaging capability, similar to a CCD in optical imaging. However, the number of pixels in our sketched case is just 3 and can be as large as 10 or so, a far cry from several million pixels obtained with CCDs.

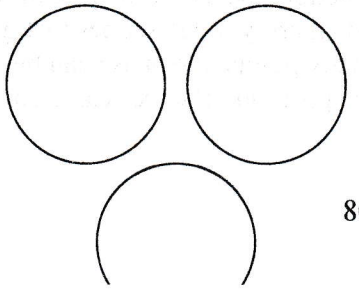

However, there are disadvantages to horn clusters:

1. The beam efficiency, the ratio of the sampled area to the total area is rather small. It decreases with increasing frequency, ν, since θ is proportional to $1/\nu$.
2. T_{sys} increases.
3. For an altitude-azimuth antenna mount, the orientation of the celestial source rotates due to the apparent diurnal motion of the sky. An equtorial mount, where one axis of the antenna points along the spin axis of the Earth would be better. However, these mounts are not often used anymore.
4. Horn clusters have a limited bandwidth.
5. Horn clusters cannot optimally illuminate the reflector aperture. For instance, the effects of scattering by feed legs or blockage by the prime focus receiver cannot be mitigated.

Because of the need to achieve a large FoV combined with multi-pixel imaging and because of the disadvantages of using horn feed clusters, electrical engineers are now working on focal plane array architectures.

There is a whole family of architectures under consideration. They have in common that they are printed circuits, kind of a 2-dim version of the 3-dim horn.

Examples of different architectures are

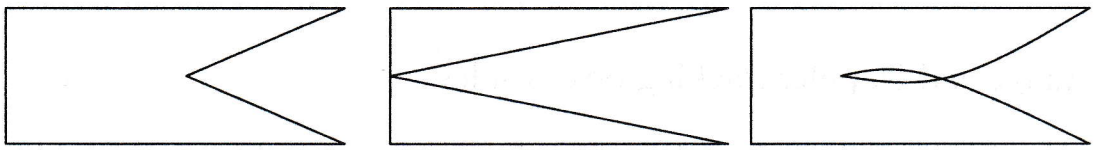

The example on the right is quite promising. It is called : Vivaldi. A number of Vivaldi antennas is put together to form an array. Vivaldi arrays have the following positive characteristics:

1. Printed circuit fabrication
2. Can be packed as closely as 0.1λ
3. Wide bandwidth of highest to lowest frequency of 5:1
4. Dual polarization capability
5. LNA can be printed on the board
6. Almost any desirable beam can be formed with digital beam formers, for instance, to block out subreflector legs of RF interference from satellites.

There is a whole "industry" out there to solve the EM properties of such antenna arrays. To compute the far-field characteristics affords massive computing power. Depending on the number of array elements there are of the order of several 100,000 free parameters to solve for.

The Vivaldi array is a big hope for interferometer arrays. Since the FWHM of interferometer arrays is very small, Vivaldi focal plane arrays may provide multiple beams and therefore a large FoV.

3.4 Receivers

Receivers for the radio range up to frequencies of 600 GHz are in general Superheterodyne systems. The heart of such a system consists of a tunable oscillator, a tunable filter and a mixer. This setup allows a range of incoming signals to be down-converted to a fixed IF.

The block diagram of a superheterodyne receiver is given on the hand-out. The first such receivers were built for AM and the figure has as an example an AM signal. Superheterodyne receivers are used in all DSN (Deep Space Network) stations. The bands used there are S, X, Ka.

4 Radiometric Tracking Techniques for DSN

4.1 Deep space radio measurements for Earth-based radio navigation

4.2 Earth-based tracking and navigation overview

4.3 Range and Doppler tracking observables

4.4 VLBI tracking observables

4.5 Future directions in radiometric tracking